ICSV19
Vilnius, Lithuania
July 08-12, 2012

SIMULATING VIBRATIONS OF A DOUBLE-LEAF PLATE WITH UNCERTAINTIES IN MATERIAL PROPERTIES AND INTERACTION BETWEEN COMPONENTS

Hyuck Chung

School of Computing and Mathematical Sciences, Auckland University of Technology, PB 92006 Auckland New Zealand,
e-mail: hchung@aut.ac.nz

Modelling the vibration of composite structures requires including the effects of uncertain material properties of individual components at mid-frequency. The purpose of this model is to predict the vibration of double-leaf plate with random parameters. One plate is excited by some force, then the vibration travels to the other plate via beams. The random parameters are the elastic modulus of the plates, and coupling conditions between components. The finite element method often used to incorporate the uncertainties in the stiffness matrix. However composite structures typically have tens of components, and formulating the stiffness matrix becomes overwhelming. Here the solution is found by minimizing the lagrangian representing the energy in the structure. The solution is expressed using the Fourier series. The coupling between components are modelled as additional energy contribution. This energy is quantified using varying resistance due to relative separation, slipping, and rotation between neighbouring components. The uncertainties then can be represented by sub-matrices in the lagrangian. As a result, the computation is simplified.

1. Introduction

This paper presents a computational modelling of vibrations of a double-leaf plates when it is subjected to some external forces. Double-leaf plates have high strength-to-weight ratio, and are used in many lightweight constructions. A simple design of a double-leaf plate has two plates sandwiching reinforcement parallel beams. There are various methods of joining the two component, such as nails and glue. The large number of distinct components and the complexity of the joints make the mathematical representation of the plate difficult (e.g., [3, 4, 6]). The distinct components, which in this case are plates and beams, require two different modelling regimes. For example, a typical finite element method (FEM) would represent the junction between a plate and a beam as 'T' shaped continuous object. This is not true in most cases because the bond at such junction would not be perfect, and also the material properties of the plate and the beams may be completely different. This paper uses an alternative way of modeling of the junctions, which are modeled how much energy is required for any particular way of bonding. The amount of energy at the junction will be large (small) if the bonding is strong (weak).

The contact conditions can be included in the formulation using the variational principle. The irregularities, including the contact conditions, can be included in the formulation using the Fourier basis expansion of the solution, which is an efficient way of finding the solution of the variational

formulation. The size of the computation is small because of the small size of the matrices related to the stiffness and the potential energies. The computation is further simplified using the simulation of the random irregularities using the predetermined PSD and simulating the normally distributed random parameters over the cosine functions. Actually it is possible to generate irregularities with any probability density function (PDF) as shown in [2]. The method here takes advantage of the known Fourier transform of the cosine functions.

The size of the linear system here is small and inverting the matrix has little computational costs. However the size of the matrix will become large as the number of components and associated randomness increase. There are many numerical techniques to optimize the inversion of the matrix and computational methods, such as parallelization. These are outside of the scope of this paper. The size of the computation will increase as the number of the components and the randomness associated with them becomes large.

This paper uses the normally distributed random parameter functions based on the given PSD. The shape of the PSD of each parameter was chosen to mimic the reality of the material's physical properties. Though it is not clear what PDF is appropriate for the stiffness of plates, shape of beams, and the coupling rigidity between the two. It is also not clear how to study the combinations of the randomness of various components. This paper only considers the effects of the randomness of one component (parameter function) at a time. For example, when the stiffness of the plate is random, other parameters are fixed.

2. Method of solution

2.1 Variational formulation of the deflection of a double-leaf plate

2.1.1 Kirchhoff plate and Euler beam models

Fig. 1 shows the depiction of a typical double-leaf plate. The top and bottom plates are modelled using the Kirchhoff plate and the beams using the Euler beam. Therefore, only the relatively small deflections (compare to their length/width) of these components are studied here. The deflec-

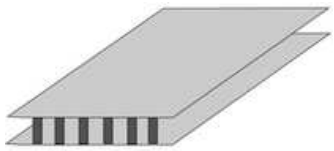

Figure 1. Schematics of a double-leaf plate.

tion of the individual components is the solutions, which will be computed in this paper. The local coordinate systems are used for each components, that is, the origin is placed at the corner of each plate, and each beam has the origin at one end. Here the simple harmonic vibration is considered, and hence the solutions will have the form $\mathbf{Re}\,[w(x,y)\exp \mathrm{i}\,\omega t]$ where ω is the radial frequency. The deflection of each component is denoted by $w_1(x,y)$, $w_2(x,j)$, and $w_3(x,y)$ for the top plate, j'th beam, and the bottom plate, respectively. Other parameters and functions will be denoted with the corresponding subscripts 1,2, or 3 for the top plate, beams, and bottom plate, respectively. For example, The thickness of the top plate is denoted by h_1, and the mass density of the bottom plate will be m_3. The length (x-direction) and the width (y-direction) are A and B, respectively. Hence the plates covers the area $(x,y) \in [0,A] \times [0,B]$, and the beams are modelled as one dimensional objects in $x \in [0,A]$. The beams have the same size, mass density and elastic modulus.

We choose the variational formulation using the lagrangian of the deflection to compute the vibration field of the structure. The vibration field of the structure is found by constructing the lagrangian of the total energy in the structure. The solution, the deformation, will be found by minimizing the lagrangian. The lagrangian for the whole structure is given by the following general form

for the deformation $\mathbf{w}$.

$$\mathcal{L}(\mathbf{w}) = \int_0^T \int_V \{\mathcal{P}(t) + \mathcal{K}(t) - \mathcal{F}(t)\}\, dvdt, \tag{1}$$

where $\mathcal{P}$ is the potential energy, $\mathcal{K}$ is the kinetic energy, and $\mathcal{F}$ is the work done to the object. The integral is taken over the volume of the elastic body and the a period of time T. Here the integral will be taken over the plates and beams.

The classical Kirchhoff (thin elastic) plate model expresses the strain energy and kinetic energy of a thin elastic plate, which has non-moving boundary, by

$$\mathcal{P}_1 = \frac{1}{2}\int_0^A \int_0^B D_1(x,y)\left|\nabla^2 w_1\right|^2 dxdy, \quad \mathcal{K}_1 = \frac{\rho_1 h_1 \omega^2}{2}\int_0^A \int_0^B |w_1(x,y)|^2\, dxdy,$$

where $D(x,y) = E_1(x,y)h_1^3/\left(12\left(1-\nu^2\right)\right)$ is the flexural rigidity and h_1, E_1, and ν are the plate thickness, Young's modulus, and Poisson ratio, respectively. Note that the effects of rotation is neglected in $\mathcal{K}_1$. The minima of Eq. (1) is the solution of the thin plate equation,

$$\nabla^2\left(D_1(x,y)\nabla^2 w_1(x,y)\right) - \omega^2 m_1 w_1(x,y) = p\left(x,y\right),$$

where $m_1 = \rho_1 h_1$ is the mass density per unit area, and p is the effective pressure acting on the plate. The above differential equation is useful when analytical solution can be considered. We however deal with irregular structural properties, and therefore the solution method is numerical. The energies for the bottom plate is given by the same formula with $\mathcal{P}_3$ and $\mathcal{K}_3$ for w_3.

The strain and kinetic energies for an Euler beam are given by

$$\mathcal{P}_2 = \frac{1}{2}\sum_{j=1}^{S}\int_0^A E_2 I\left|w_{2xx}(x,j)\right|^2 dx, \quad \mathcal{K}_2 = \frac{\rho_2 h_2 \omega^2}{2}\sum_{j=1}^{S}\int_0^A |w_2(x,j)|^2\, dx,$$

where E_2 and I are the Young's modulus and the moment of inertia of the beam, and $\rho_2$and h_2 are the mass density per unit length and the thickness of the beam, respectively.

2.1.2 Coupling conditions

In addition to the strain and kinematic energy, we include the energy contributions from the coupling of top/bottom plate and the beam due to the discrepancy in the displacement of the two components. For example, the coupling between the top plate and the beams is given by

$$\mathcal{P}_{1,2}^{\text{sep}} = \frac{1}{2}\sum_{j=1}^{S}\int_0^A \sigma_{\text{sep}}\left(x,j\right)\left|w_1\left(x,y_j\right) - w_2\left(x,j\right)\right|^2 dx, \tag{2}$$

$$\mathcal{P}_{1,2}^{\text{slip}} = \frac{1}{2}\sum_{j=1}^{S}\int_0^A \sigma_{\text{slip}}\left(x,j\right)\left|h_1 w_1'\left(x,y_j\right) + h_2 w_2'\left(x,j\right)\right|^2 dx, \tag{3}$$

$$\mathcal{P}_{1,2}^{\text{rot}} = \frac{1}{2}\sum_{j=1}^{S}\int_0^A \sigma_{\text{rot}}\left(x,j\right)\left|w_1'\left(x,y_j\right) - w_2'\left(x,j\right)\right|^2 dx, \tag{4}$$

where $'$ indicates the x-derivative and σ_{sep}, σ_{slip}, and σ_{rot} are the Hooke's constants for springs resisting relative separation, slipping, and rotation of the coupled layers, respectively. These functions are defined along the beams, and thus functions of x. The subscripts (l,j) indicate the interaction between either top plate and beams ($(l,j) = (1,2)$), or bottom plate and the beams ($(l,j) = (3,2)$). Note that the stiffness of these springs may vary along the coupling layer and from one layer to another. The simpler model of coupling between the plate and the beams may let the separation constant σ_{sep} become infinite, that is the separation is zero and the plate and the beams are always in contact. The total potential energy, $\mathcal{P}$, is the sum of all potential energies from individual layers and coupling between layers.

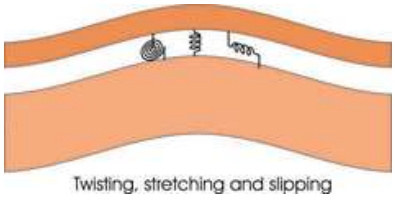

Figure 2. Depiction of the model for the coupling conditions. The springs give the resistance to the horizontal (left), vertical (centre), and rotational (right) movements.

2.2 Computation method of solutions

2.2.1 The Fourier expansion of the solution

The method of solution chosen in this paper is the Fourier expansion method, which is ideal because of the rectangular shape of the structure. Furthermore the boundary of the plate is assumed to be simply supported. Thus the basis functions are sine-functions, further simplifying the solution. Different basis functions must be chosen when the boundary conditions are different. There are a few example sets of basis functions shown in [5] for free or clamped boundaries. Whatever the basis functions may be, a linear system of equations for the coefficients of the expansion over the chosen basis functions. Hence the method of solution shown here will be applicable.

The deflection of the top, bottom plates, and beams are written by

$$w_1(x,y) = \sum_{m,n=1}^{N} C_{mn}^{(1)}\phi_m(x)\psi_n(y), \quad w_3(x,y) = \sum_{m,n=1}^{N} C_{mn}^{(3)}\phi_m(x)\psi_n(y), \quad w_2(x,j) = \sum_{m=1}^{N} C_{mj}^{(2)}\phi_m(x),$$

for $j = 1, 2, ..., S$, respectively, where the basis functions are $\phi_m(x) = \sqrt{2/A}\sin k_m x$, and $\psi_n(y) = \sqrt{2/B}\sin \kappa_n y$, and the wavenumbers are given by $k_m = \pi m/A$ and $\kappa_n = \pi n/B$. Note that the basis functions are orthonormal. The positions of the joists are given by $y = y_j$, $j = 1, 2, ..., S$. Note that the number of terms in the series has already been truncated to N to construct the finite system for the numerical computation. The operations are then expressed using the column vectors of the coefficients,
$\mathbf{c_1} = \left(C_{11}^{(1)}, C_{21}^{(1)}, \cdots, C_{NN}^{(1)}\right)$, $\mathbf{c_2} = \left(C_{11}^{(2)}, C_{21}^{(2)}, \cdots, C_{NS}^{(2)}\right)$, and $\mathbf{c_3} = \left(C_{11}^{(3)}, C_{21}^{(3)}, \cdots, C_{NN}^{(3)}\right)$. The variational formulation then becomes

$$\frac{1}{2}\begin{bmatrix}\mathbf{c}_1\\ \mathbf{c}_2\\ \mathbf{c}_3\end{bmatrix}^{\mathrm{t}} \mathbf{L} \begin{bmatrix}\mathbf{c}_1\\ \mathbf{c}_2\\ \mathbf{c}_3\end{bmatrix} = \mathbf{f}^{\mathrm{t}} \begin{bmatrix}\mathbf{c}_1\\ \mathbf{c}_2\\ \mathbf{c}_3\end{bmatrix}.$$

where $\mathbf{L}$ is the matrix from the integrals and $\mathbf{f}$ is the vector of the external forcing, whose elements are given by $\int_0^A \int_0^B f(x,y)\phi_m(x)\psi_n(y)\,dx$ with zero padding for the parts corresponding to $\mathbf{c}_2$ and $\mathbf{c}_3$. In §2.2, the forcing is set to be a point forcing, that is, $f(x,y) = \delta(x - x_0, y - y_0)$ for some fixed point (x_0, y_0), which makes the integrals unnecessary. The following subsections will give details how the elements of $\mathbf{L}$ are obtained.

2.2.2 Contact conditions between the plates and the beams

The irregularity in bonding between floor and joists can be included by changing the function $\sigma_{\text{slip}}(x)$, $\sigma_{\text{rot}}(x)$, and $\sigma_{\text{sep}}(x)$ in Eq. (3). In this paper, only $\sigma_{\text{slip}}(x)$ is varied for the numerical simulations.

Substituting the Fourier series expansion for the deflections w_1 and w_2 to Eq. (3) gives

$$\mathcal{P}_{1,2}^{\text{slip}} = \sum_{j=1}^{S} \int_0^A \sigma_{\text{slip}}(x,j) \left| h_1 \sum_{m,n=1}^{N} k_m C_{mn}^{(1)} \varphi_m(x)\psi_n(y_j) + h_2 \sum_{m=1}^{N} k_m C_{mj}^{(2)} \varphi_m(x) \right|^2 dx$$

where $\varphi_m(x) = \sqrt{2/A}\cos k_m x$. Then the above integral will be obtained by computing

$$\int_0^A \sigma_{\text{slip}}(x,j)\varphi_m(x)\varphi_{m'}(x)\,dx = \frac{1}{A}\int_0^A \sigma_{\text{slip}}(x,j)\left(\cos\frac{\pi(m-m')}{A}x - \cos\frac{\pi(m+m')}{A}x\right)dx.$$

Notice that this integral is simply the Fourier cosine coefficients of the function $\sigma_{\text{slip}}(x,j)$, which can be computed using the fast Fourier transform (FFT).

2.2.3 Elastic modulus of the plates

Substituting the series expansion for $w_1(x,y)$ to equation for $\mathcal{P}_1$ leads to vector and matrix expression for the strain energy of the top plate. Let the function D_1 be separated into $D_1(x,y) = D_{\text{c1}} + d_1(x,y)$ where D_{c1} is constant. The elements of the matrix $\mathbf{L}$ due to the the varying stiffness $D_1(x,y)$ are computed using the integral

$$\sum_{m,n,m',n'=1}^{N} \int_0^A \int_0^B d_1(x,y) C_{mn}^{(1)} C_{m'n'}^{(1)} \left(k_m^2 + \kappa_n^2\right)\left(k_{m'}^2 + \kappa_{n'}^2\right)\phi_m(x)\phi_{m'}(x)\psi_n(y)\psi_{n'}(y)\,dxdy.$$

The constant stiffness D_{c1} will give us a diagonal matrix with its element $(k_m^2 + \kappa_n^2)^2$ because of the orthogonality of the functions $\{\phi_m\}$ and $\{\psi_n\}$. Note that the parts of the lagrangian matrix related to the beams will have diagonal elements only because the stiffness of them is assumed to be constant. Again the above integral is the formula for the 2d Fourier coefficients for the function $d_1(x,y)$, which can be found using the 2d FFT. The length of the transform must be double that of the sampled data of $d_1(x,y)$. Furthermore, the products of *cosine* components are obtained by taking the real part of the FFT in x and y directions. The contribution from the bottom plate can be derived using the same formula with w_3.

2.2.4 Shape of the joists

The numerical computation with twisting beams is not carried out here, and only the brief derivation of the linear system will be given. In order to include not-so-straight shape of beams, we here make a few assumptions and keep the model simple. The strain energy of the beams are computed in the same way as before by integrating over the x from 0 to A. The shape of j'th beam is denoted by the function of x, $\theta_j(x)$. Thus the contact between the top plate and the beam is given by $y_j + \theta_j(x)$. We first take the Taylor expansion of the modes at the contact curves and omit the higher terms because $\theta_j(x)$ is assumed small, that is, $\psi_n(y_j + \theta_j(x)) \approx (1 + \kappa_n\theta_j(x))\,\psi_n(y_j)$. Then the displacement of the plate at the locations of the beams, denoted by B_j are given by

$$w_1 = \sum_{m,n=1}^{N} (1 + \kappa_n\theta_j(x))\, C_{mn}^{(1)}\phi_m(x)\psi_n(y_j), \quad \text{for } (x,y) \text{ where the beams are.}$$

The energy contributions $\{\mathcal{P}_{i,j}\}_{(i,j)=(1,2),(2,3)}$ are now calculated from the above two expressions. For example, the potential energy due to the slippage at the twisting beams is given by

$$\mathcal{P}_{1,2}^{\text{slip}} = \frac{1}{2}\int_0^A \sigma_{\text{slip}}(x,j)\left| h_1 \sum_{m,n=1}^{N} C_{mn}^{(1)}\left(k_m + k_m\kappa_n\theta_j(x)\right)\phi_m(x)\psi_n(y_j) + h_2\sum_{m=1}^{N} k_m C_{mj}^{(2)}\phi_m(x)\right|^2 dx$$

Note that the higher order terms have been omitted. The above integral can be expressed using vector operations between $\mathbf{c}_1$ and $\mathbf{c}_2$ as shown in the previous section.

2.3 Simulation of irregularities based on power spectral density

The parameter functions with any PDF can be simulated using the method given in [2]. When the PSD is given by $P_\sigma(x)$, the realizations of the parameter function $\sigma(x)$ with PDF $p_\sigma(x)$ are derived by the following procedures. The parameter function can be expressed by

$$\sigma(x) = \sqrt{2/M} \sum_{i=1}^{M} Q_i \cos\left(2\pi F_i x + \Phi_i\right) \tag{5}$$

where the mean of $\sigma(x)$ is zero for all $x \geq 0$. The PDF of the frequency F_i is determined by $p_F(|f|) = 2/E\left[Q^2\right] P_\sigma(f)$, for $-1/2 \leq f \leq 1/2$, where P_σ is the desired PSD of σ, which in this is given by a smooth *hump*-function (see Fig. 3). Thus the random variable F_i has Gaussian distribution. The PDF for Q is given by

$$p_Q(q) = q \int_0^\infty \left(\psi_\sigma(\sqrt{M/2}v)\right)^{1/M} J_0(qv) v \, dv$$

where ψ_σ is the characteristic function, $p_Q(q)$ is the PDF of the amplitude Q_i and J_0 is the Bessel function of the first kind of order zero. The rigorous explanation of the above items is given in the Appendix of [2]. Here the Gaussian distribution is chosen as the target PDF, and thus Q_i is the Rayleigh random variable.

The 2 dimensional function $d_1(x, y)$, the deviation from the ideal stiffness, can be similarly simulated using the expansion

$$d_1(x, y) = \sum_{i,j=1}^{M} Q_i R_j \cos\left(2\pi F_i x + \Phi_i\right) \cos\left(2\pi G_j y + \Psi_j\right) \tag{6}$$

where the coefficients $\{Q_i, R_j\}$ are random variables with the PDFs given by the method above, which again are the Rayleigh random variables. The phase Φ_i and Ψ_j are uniformly distributed random values in $[-\pi, \pi]$. The frequencies F_i and G_j are again Gaussian random variable.

3. Computation results and analysis

3.1 Simulation of $\sigma(x)$ and $D(x, y)$ from PSD

The functions $\sigma_{\text{slip}}(x)$ represents the qualitative bonding rigidity and is created for the convenience of modelling, and thus cannot be measured directly. However, it may be reasonable to assume $\sigma_{\text{slip}}(x)$ to have Gaussian distribution. The simple Gaussian PDF[1] in 1 and 2 dimensional spaces will be considered for the PSD of $\sigma_{\text{slip}}(x, j)$, $d_1(x, y)$ and $d_3(x, y)$. The realizations $\sigma_{\text{slip}}(x)$ and $d_1(x, y)$ are shown in Figs. 3 and 4 using the methods given by Eqs. (5) and (6) in §2.3. Two sets of slippage and stiffness with two periods of variations along the beams and over the plates have been used. The variance of the simulated functions are set to 20% and 2% of the average constant for the slippage and the stiffness, repectively.

3.2 Surface vibration levels

Fig. 5 shows the root mean square of the surface velocity at the frequencies from 150Hz to 250Hz. The slippage is randomized for Figs. 5(a) and (b), and the stiffness is randomized for Figs. 5(c) and (d). Figs. 5(a) corresponds to the slippage given by Fig. 3(a,b), and Fig. 5(b) does to Fig. 3(c,d).

[1]The method of [2] allows any PDF for the frequency. The random variables can be generated using the inverse of the cumulative distribution function of the uniform random variable.

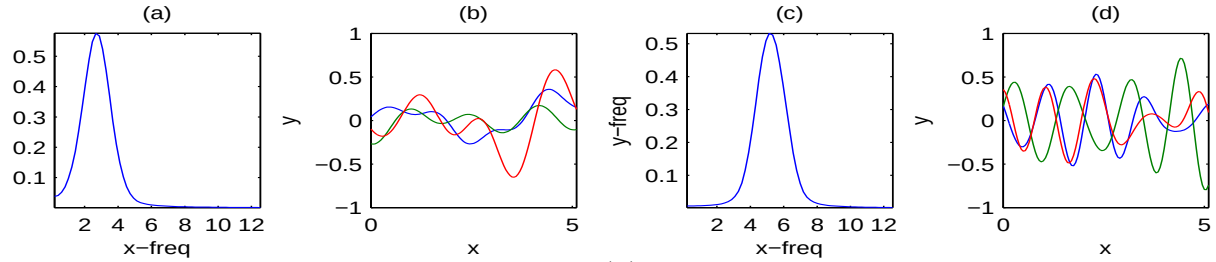

Figure 3. The PSD ((a) and (c)) of the simulated $\sigma_{\text{slip}}(x)$ and a few typical realizations ((b) and (d)) of $\sigma_{\text{slip}}(x)$.

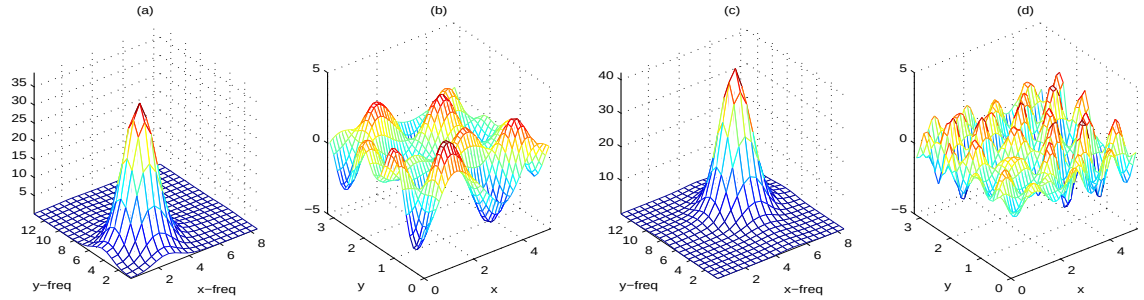

Figure 4. The PSD ((a) and (c)) of the simulated $d_1(x, y)$ and a typical realization ((b) and (d)) of $d_1(x, y)$.

The randomness of the slippage affects the surface velocity mostly near the resonant frequencies. However, there is little effects showing between 220 and 240Hz, even thought there are several resonances in that range. The stiffness for Figs. 5(c) and (d) are from the ones shown in Fig. 4(a,b) and (c,d), respectively. The random stiffness with higher spacial frequency affects the higher frequency range. The average resonant frequency peaks are smoothed when the stiffness is randomized. Furthermore the variance of the vibration level is nearly uniform after 220Hz. In both slippage and stiffness cases, the lower variations of the random functions lead to slightly more smoothed out vibration levels.

Figs. 6 and 7 show the distributions of the variance of the surface deflection of the top plate when slippage and stiffness are randomized, respectively. There is little variance at a lower frequency. At the higher frequencies, the location of the beams affects the variance distribution. However the variance is not distributed evenly. The slippage affects lower frequency vibrations than it does the higher frequency ones as shown in Fig. 5(a,b) with respect to the mode shape. The stiffness affects the higher frequency vibrations. The variance distribution become uneven.

The parameters for the beams and the plates are chosen from the nominal values for plywood and timber beams, $E_1 = 10^9$Pa, $m_1 = m_2 = M_3 = 500$kg/m^3, $A = 5.1$m, $B = 3.2$m, $h_1 = h_3 = 0.015$m, $h_2 = 0.3$m, $\nu = 0.3$ $y_j = jB/8$, $j = 1, 2, ..., 7$, and the width of the beams is 0.045m. The average slippage constant is 3×10^7N/m, which was determined from the experiments in [1]. The

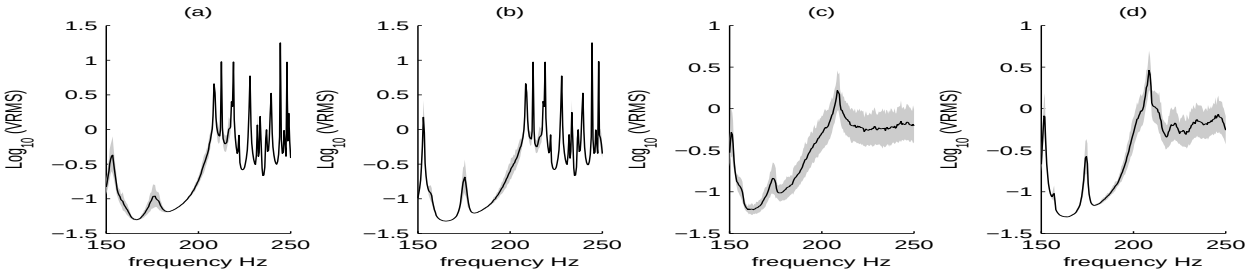

Figure 5. The average root-mean-square of the surface velocity from 150Hz to 250Hz when the slippage resistance (a,b) and stiffness (c,d) are randomized. The variance is shown by the grey area.

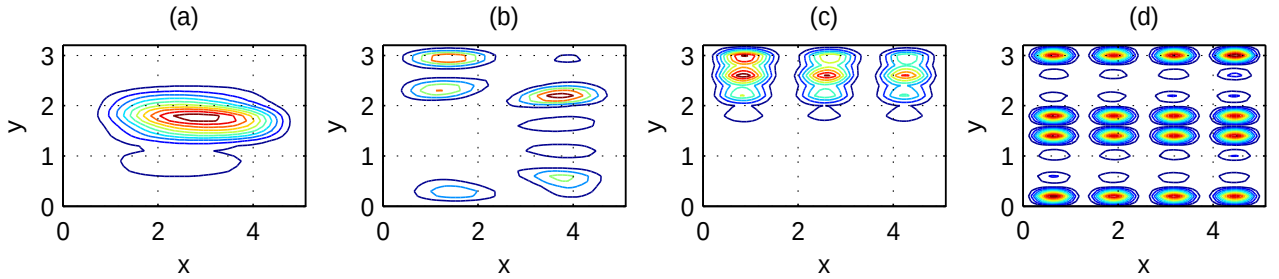

Figure 6. The distribution of the variance of the surface deflection at (a) 100Hz, (b) 150Hz, (c) 200Hz, and (d) 250Hz when the slippage resistance is randomized.

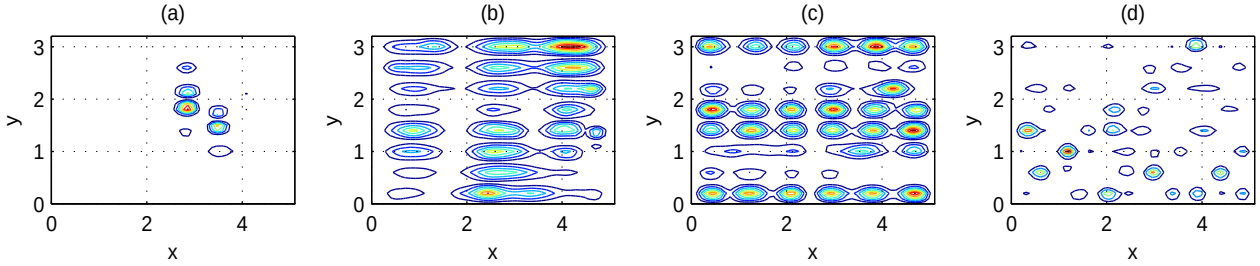

Figure 7. The distribution of the variance of the surface deflection at (a) 100Hz, (b) 150Hz, (c) 200Hz, and (d) 250Hz when the stiffness of the top and the bottom plates is randomized.

location of the forcing is $(2.85, 2.1)$.

4. Conclusions and summary

Even with the relatively simple model with two varying functions, slippage and stiffness, the simulations generate a great deal of data, which makes analysing the effects of the randomness difficult. It is not clear how the combinations of particular randomness would affect the whole vibrations the most or the least. The numerical simulations show that the irregularities (variations along the beam or within the plate) affects the whole vibration. Thus the modelling of composite structure, even this moderately complex double-leaf plate, require the random irregularities to be taken into account in order to make realistic estimates. The irregular features, stiffness of the plates, shape of the beams and junction between the plates and the beams, are modelled using the variational principle.

REFERENCES

[1] Chung, H. and Emms, G., *Fourier series solutions to the vibration of rectangular lightweight floor/ceiling structures*, ACTA Acustica united with Acustica, 94(3) 401-409 (2008).

[2] Kay, S., *Representation and generation of non-gaussian wide-sense stationary random process with arbitrary PSDs and a class of PDFs*, IEEE Trans. Signal Processing, 58(7) 3448–3458 (2010).

[3] Ngah, M.F. and Young, A., *Application of the spectral stochastic finite element method for performance prediction of composite structures.* Composite Structures, (2007) 78, pp. 447–456

[4] Ren, Y.J. and Elishakoff, I., *New results in finite element method for stochastic structures.* Computers and structures, (1998) 67, pp. 125–135.

[5] Shames, I.H. and Dym, C.L., *Energy and Finite Element Methods in Structural Mechanics*, Taylor and Francis Publishers, New York, 2003.

[6] Yu, G.L., Wang, Y.S. and Lan, J., *Vibration localization in disordered periodically stiffened double-leaf panels.* Arch. Appl. Mech., (2010) 80, pp. 687–697.